



16^{èmes} Journées de l'Hydrodynamique

27-29 novembre 2018 - Marseille



CENTRALE
MARSEILLE



ESTIMATION DE L'ETAT DE MER EN TEMPS REEL A PARTIR DE MESURES INERTIELLES DES MOUVEMENTS D'UN NAVIRE

REAL-TIME SEA-STATE ESTIMATION FROM INERTIAL MEASUREMENTS OF A SHIP'S MOTIONS

S.T GRILLI⁽¹⁾, J.M. DAHL⁽¹⁾, A.R. GRILLI⁽¹⁾, S.C. STEELE⁽¹⁾
grilli@uri.edu ; jmdahl@uri.edu ; annette_grilli@uri.edu ; ssteele@uri.edu

⁽¹⁾Department of Ocean Engineering, University of Rhode Island, Narragansett, RI, USA

Résumé

Dans les études standards de tenue à la mer, les mouvements d'un navire supposé rigide sont calculés en réponse à des vagues irrégulières, correspondant à un état de mer défini par sa hauteur significative H_s , période du maximum spectral T_p , direction dominante θ_0 , et type de spectre (e.g., JONSWAP). Dans ce travail, sur la base de telles simulations de tenue à la mer, un Réseau Neuronal (RN) est configuré afin de procéder à l'inverse : à partir des mouvements d'un navire, mesurés par exemple à l'aide d'un système inertiel embarqué, ce RN estimera les paramètres de l'état de mer (H_s, T_p). La motivation principale de ce projet est de développer une méthode à bas coût afin que des remorqueurs de haute mer (destinés à transférer du cargo) puissent estimer l'état de mer et ainsi éviter d'opérer dans des conditions dangereuses. Cependant, la même méthode pourrait être appliquée à des navires génériques de haute mer, pour obtenir des mesures locales et continues de l'état de mer à des fins scientifiques ou autres.

Summary

In standard seakeeping simulations, the rigid body motions of a ship are computed in response to incident irregular waves, corresponding to a sea state defined by its significant wave height H_s , peak spectral period T_p , dominant direction θ_0 , and spectrum type (e.g., JONSWAP). In this work, on the basis of such seakeeping simulations, a Neural Network (NN) is trained to perform the inverse problem : given a time series of ship motions, such as that measured with an onboard inertial system, the NN will estimate key sea state parameters (H_s, T_p) based on the observed ship motions. The main rationale for this work is to develop a low cost method for small Naval vessels to estimate local sea state conditions in order to avoid operations in dangerous sea states, however the same techniques could be applied in general to transiting vessels to obtain local and continuous sea state measurements for general science purposes or other uses.

I – Introduction

In state-of-the-art naval hydrodynamics models, a ship’s rigid body motions in irregular sea-states are typically computed based on potential flow theory and, rather than tackling the fully nonlinear problem, which is still highly computationally costly, a linear model is used with some ad-hoc nonlinear corrections, in particular for hydrostatic restoring forces, moments, and viscous damping of ship motions. There exist many commercial codes based on these principles, such as AQWA (<http://osk-shiptech.com/Toolbox/AQWA>), in which potential flow equations are typically solved with a higher-order Boundary Element Method (BEM). With such models, given the ship geometry and characteristics of mass and inertia, one first solves up to 6 radiation problems (for up to 6 degrees-of-freedom (dofs) : 3 translations and 3 rotations) in which the ship has a forced periodic motion of unit amplitude; this is repeated for a large number of frequencies (ω_n ; $n = 1, \dots, N_\omega$), which in each case provides the ship’s linear added mass $A_{ij}(\omega_n)$ and damping $B_{ij}(\omega_n)$ matrices, respectively (with in general $i, j = 1, \dots, 6$). For each of these frequencies and for N_w incident wave directions θ_w ($w = 1, \dots, N_w$), a series of diffraction problems are solved with the model, assuming a unit incident wave amplitude and considering the ship is fixed, which provides the Froude-Krylov (FK) and diffraction forces (and moment) applied to the ship, $(R_i^w(\omega_n), \alpha_i^w(\omega_n))$, for its module and phase, respectively.

Given an irregular sea state defined by its significant wave height H_s , peak spectral period T_p , dominant direction θ_0 , and spectrum type (e.g., JONSWAP (JS)), the ship instantaneous motions $\zeta_i(t)$ are then obtained by solving differential equations expressing momentum conservation for each of the selected dof of rigid body motion (up to 6). These equations include mass/inertia (plus added mass/inertia), radiative and viscous damping, hydrostatic restoring, total FK forcing, and memory terms. The latter are integrals convolving the impulse response function $K_i(t)$ associated with each dof of the ship and all its previous states of motion.

In this work, we develop a methodology, based on a pattern recognition Artificial Intelligence (AI) method, to perform the opposite task, i.e., given a time series of ship motions, such as measured with an onboard inertial system, the AI method should provide an accurate estimate of key sea state parameters (H_s, T_p). The main rationale for this work was to develop a low cost method for slow moving, barge-like, workboats (e.g. tug boats) to estimate real time local sea state conditions, in order to avoid operations in dangerous sea states. These types of workboats can encounter strong interactions when operating closely with another vessel or floating structure, hence safe operations are highly affected by the sea state. The same approach could also be applied to generic transiting vessels, to obtain local and continuous sea state measurements for general science purposes or other uses.

To perform this “sea state inversion”, a Neural Network (NN) was trained using a large number of seakeeping simulations (i.e., simulated time series of ship motions) obtained for a ship with known characteristics, and for many specified sea states of given parameters (H_s, T_p) originating from a specific direction (e.g., head sea). For the sake of illustrating the methodology, the approximate characteristics of a barge-like tug boat are used in the model, for which time domain seakeeping simulations are performed. A NN is trained based on the output time series of the model and is then validated using times series not used in training the model. By repeating this operation, the ability of the NN to accurately predict the sea state is assessed. While the interrogation of the NN must be done in real time on the physical ship, the more time consuming and computationally demanding NN training phase can be performed a priori using the accurate ship dynamics model.

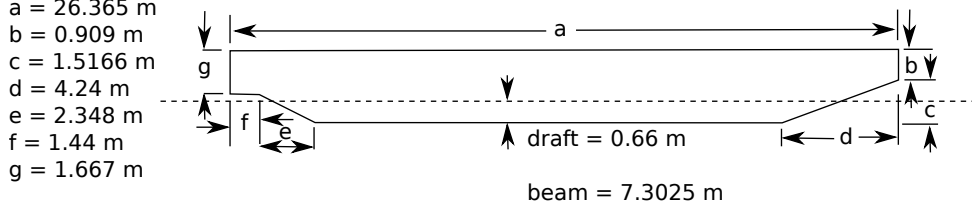


FIGURE 1 – Approximate hull form used in the present study with approximate dimension : length $L = 26.37$ m, draft $D = 0.66$ m, and beam $B = 7.30$ m.

II – Model Development

A time-domain seakeeping model is derived to predict the heave, pitch, and roll motion of the vessel shown in Fig. 1, given an input wave spectrum based on specific sea state conditions. The model follows the procedures previously successfully demonstrated in the development of a semi-analytical model for wave energy conversion systems [3]. In particular, the model is accelerated by using the Prony approximation method proposed by Babarit and Clément [1], for computing the convolution memory terms in the ship equations of motion. As a note, the present model assumes zero forward speed of the vessel, however future work will adjust the model to accommodate the response of the model to the encounter frequency of waves at forward speed.

II – 1 Equations of motion

The ship motion along each dof (heave, roll, and pitch ; $i = 3, 4, 5$ in the standard definition) is modeled by a (linear or angular) momentum conservation equation, with a mass and constant (infinite frequency) added mass inertial term, a memory term expressing the linear radiative damping and transient added mass effects, nonlinear hydrostatic restoring force, hydrostatic coupling between motions, a nonlinear viscous drag term (proportional to velocity squared), and a linear excitation force, resulting from summing the Froude-Krylov and diffraction forces for each wave frequency component ($n = 1, \dots, N_\omega$) in a specified JS wave spectrum of characteristics (H_s, T_p) , here defined as unidirectional and incident from direction θ_w . The equation of motion for each ship dof $\zeta_i(t)$ ($i = 3, 4, 5$) is then :

$$(M_{ii} + A_{ii}(\infty)) \ddot{\zeta}_i + \int_0^t K_i(t-\tau) \dot{\zeta}_i d\tau + C_{ii}(\zeta_i - \eta) \zeta_i + \sum_{j \neq i} C_{ij} f(\zeta_j) + b_{Di} \dot{\zeta}_i |\dot{\zeta}_i| = F_i^w(t), \quad (1)$$

where, M_{ij} denotes the ship mass and inertia matrix, $C_{ij}(\zeta_i - \eta)$ the nonlinear hydrostatic restoring force/moment (per unit displacement) with $f(\zeta_j) = \zeta_j$ for $j = 3$ and otherwise $f(\zeta_j) = \sin \zeta_j$, and $b_{Di} = (1/2)\rho C_{Di} S_{wi}$ the nonlinear viscous damping term, with ρ the fluid density, C_{Di} a total drag coefficient, and S_{wi} a relevant wetted surface area.

Given a set of wave amplitudes $a_n(\omega_n) = \sqrt{2E(\omega_n)\Delta\omega}$, extracted from a discretized wave frequency spectrum $E(\omega)$, with discretization $\Delta\omega$, and random phases $\varphi_n \in [0, 2\pi]$, the instantaneous wave surface elevation is expressed as :

$$\eta(t) = \sum_{n=1}^{N_\omega} a_n(\omega_n) \cos(\omega_n t + \varphi_n), \quad (2)$$

with the wave excitation force (including the FK and diffraction components) defined as :

$$F_i^w(t) = \sum_{n=1}^{N_\omega} a_n(\omega_n) R_i^w(\omega_n) \cos(\omega_n t + \alpha_i^w(\omega_n) + \varphi_n), \quad (3)$$

Based on linear seakeeping theory, for each degree of freedom ($i = 3, 4, 5$), the impulse response functions, $K_i(t)$, used in evaluating the memory dependent force on the vessel can be defined based on the frequency dependent added mass and damping coefficients, as in Eqs. (1) :

$$K_i(t) = -\frac{2}{\pi} \int_0^\infty (A_{ii}(\omega) - A_{ii}(\infty)) \omega \sin(\omega t) d\omega = \frac{2}{\pi} \int_0^\infty B_{ii}(\omega) \cos(\omega t) d\omega, \quad (4)$$

As noted in earlier work [1, 3], the numerical solution in the time domain of the system of coupled nonlinear integro-differential momentum equations Eqs. (1-4), governing the ship motion in a specified sea state, is computationally demanding due to the presence of the convolution integrals that describe the effects of the ship's earlier states of motion on its current motion.

To overcome this difficulty, as proposed by [1], the Prony approximation method is used to transform the memory terms into a set of differential equations that solve for the Prony coefficients, which are used to approximate the impulse response function, thus yielding a larger system of ordinary differential equations (ODEs). The Prony approximation defines the impulse response function to be approximated by a Prony series, or a series of decaying complex exponential functions :

$$K_i(t - \tau) = \sum_{p=1}^P \beta_{p,i} e^{S_{p,i}(t-\tau)}, \quad (5)$$

with P the selected number of complex Prony coefficients $\beta_{p,i}$ and $S_{p,i}$. The Prony coefficients are obtained by evaluating a least squares fit of the Prony function to each function $K_i(t)$ calculated with Eq. (4), for the selected Prony coefficients. This procedure may be evaluated for several values of a P to determine the most accurate approximation for a given set of functions $K_i(t)$. Note that it is possible to evaluate this approximation using either the added mass or damping form of Eq. (4), however we use the damping form of the equation as it is found to be more accurate for short term memory effects (near $t = 0$). Based on this definition, for each dof, the memory term in Eqs. (1) is approximated as :

$$\int_0^t K_i(t - \tau) \dot{\zeta}_i(\tau) d\tau = \sum_{p=1}^P \beta_{p,i} \int_0^t e^{S_{p,i}(t-\tau)} \dot{\zeta}_i(\tau) d\tau = \sum_{p=1}^P \beta_{p,i} I_{p,i}, \quad (6)$$

$$I_{p,i} \equiv e^{S_{p,i}t} \int_0^t e^{-S_{p,i}\tau} \dot{\zeta}_i(\tau) d\tau \quad (7)$$

$$\dot{I}_{p,i} = S_{p,i} I_{p,i} + e^{S_{p,i}t} \frac{d}{dt} \left\{ \int_0^t e^{-S_{p,i}\tau} \dot{\zeta}_i(\tau) d\tau \right\} = S_{p,i} I_{p,i} + \dot{\zeta}_i, \quad (8)$$

Based on Eqs. (5-8), the ship motion is computed as a function of time for each dof by solving the system of coupled second-order ODEs (1) simultaneously with $2P$ first-order real ODEs (8) for the P complex Prony coefficients $I_{p,i}$ of each degree of freedom

$i = 3, 4, 5$. To apply a numerical ODE solver, this system is conveniently recast into one of coupled first-order ODEs as ($i = 3, \dots, 5; p = 1, \dots, P$),

$$\dot{\zeta}_i = V_i \quad (9)$$

$$\dot{V}_i = -\frac{1}{m_i} \left\{ \sum_{p=1}^P \beta_{p,i} I_{p,i}(V_i, t) + F_{H,i}(\zeta_i) + b_{Di} V_i |V_i| - F_i^w(t) \right\} \quad (10)$$

$$\dot{I}_{p,i} = S_{p,i} I_{p,i}(V_i, t) + V_i, \quad (11)$$

with $m_i = (M_{ii} + A_{ii}(\infty))$ and,

$$F_{H,i}(\zeta_i) = C_{ii}(\zeta_i - \eta(t))\dot{\zeta}_i + \sum_{j \neq i} C_{ij} f(\zeta_j) \quad (12)$$

For a specified sea state (with JS spectrum $E(\omega)$), the system of ODEs (9-12) is solved using one of Matlab's standard ODE solvers, based on an optimized Runge-Kutta method, for either a fixed maximum duration t_{max} or one that is equal to a specified multiple of T_p (e.g., 100). Once the solution is obtained and provided in terms of $\zeta_i(t)$ ($i = 3, 4, 5$), various other parameters such as ship velocity and acceleration $[\dot{\zeta}_i(t), \ddot{\zeta}_i(t)]$, as well as force components, can easily be computed as a function of time using the same equations with the known solution.

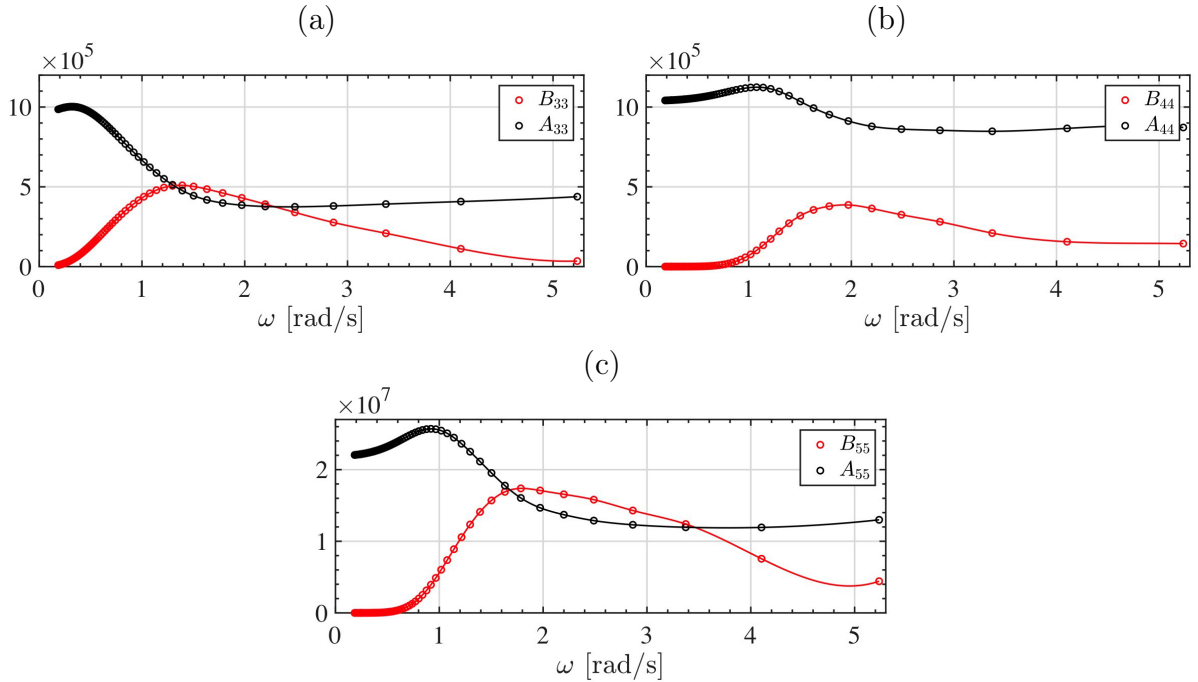


FIGURE 2 – Added mass and damping coefficients calculated for the warping tug with AQWA (symbols) in : (a) heave ; (b) roll ; and (c) pitch. Lines are spline fits through data.

III – Application of the seakeeping model to the vessel

For the purpose of illustrating the sea state inversion methodology, the time series of heave, roll and pitch motions, are first computed for a series of sea states, using the approximate characteristics of the boat shown in Fig. 1.

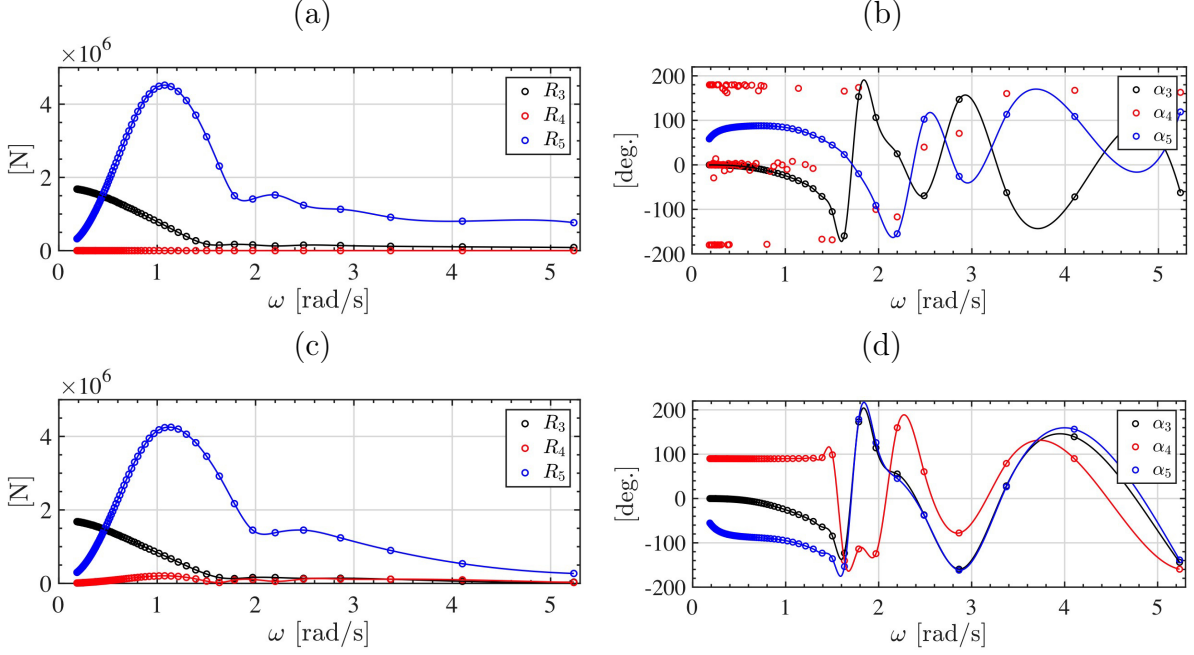


FIGURE 3 – (a,c) Module R_i and (b,d) phase α_i ($i = 3, 4, 5$) of total excitation forces calculated as a function of angular frequency for the warping tug with AQWA in heave, pitch, and roll, for a : (a,b) head sea at 180° , and (c,d) and oblique sea at 27° .

III – 1 Linear seakeeping results

The general dimensions of the vessel are length $L = 26.37$ m, draft $D = 2.43$ m, and beam $B = 7.30$ m. The density of water is assumed to be $\rho = 1,025$ kg/m³. Using the approximate geometry and mass/inertia characteristics M_{ij} of the boat and its linear hydrostatic restoring coefficients C_{ij} , linear seakeeping simulations were run using AQWA at zero forward speed, that provided results for $N_w = 100$ frequencies over the range $\omega_n \in [0.185 - 5.236]$ rad/s (period $T = 34.0 - 1.2$ s respectively), and at $N_w = 21$ wave incident angles $\theta_w \in [0^\circ - 180]^\circ$, by increments of 9° . For use in the above time domain model, data was interpolated at the desired frequencies and angles.

The results from AQWA include frequency dependent added mass coefficients $A_{ij}(\omega)$, frequency dependent damping coefficients $B_{ij}(\omega)$, and for each direction, w , and the module, $R_i^w(\omega)$ and phase, $\alpha_i^w(\omega)$, of the total excitation force. Fig. 2 shows examples of linear added mass and damping values for the vessel, as a function of frequency in heave, roll, and pitch. Fig. 3 shows the module and phase of the total excitation forces in heave, pitch, and roll, for the case of head sea (180°) and an oblique sea, at 27° . Fig. 4 shows the calculated heave, roll, and pitch impulse response functions, using the standard Eqs. (4) based on AQWA calculated $B_{ij}(\omega)$ results, together with the corresponding ‘‘Prony’’ curve fit with $P = 4$ complex coefficients. These approximations match well with the impulse response curves for the first few seconds of larger ship motions, where the memory term is most important.

The sea state is represented by a unidirectional JS spectrum $E(\omega)$, with parameters (H_s, T_p) ; in the following, the spectral peakedness parameter is set to its standard average value, $\gamma = 3.3$. Future work will consider directional seas and thus JS spectra with a directional spreading function. Fig. 5 shows an example of a JS spectrum calculated for $H_s = 2$ m and $T_p = 8$ s. Each sea state’s spectrum is discretized into $N_w = 200$ frequencies, equally spaced over the interval where the spectrum has energy larger than 0.1% of its

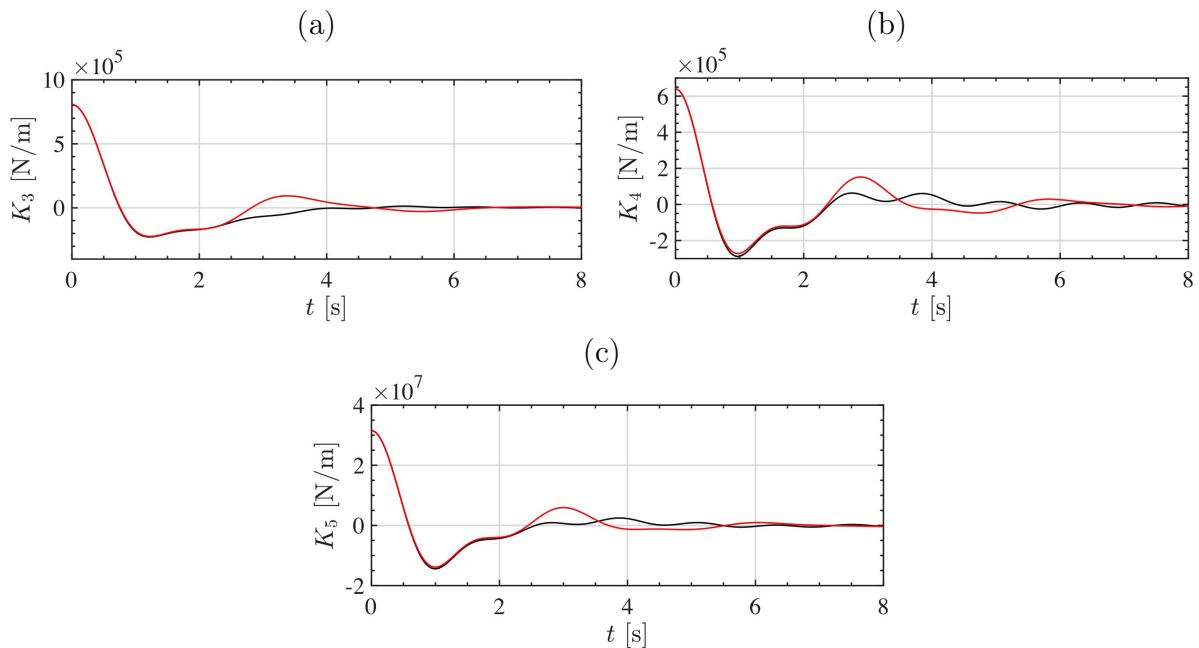


FIGURE 4 – Impulse response functions K_i ($i = 3, 4, 5$) computed with Eq. 4 (black) (using Fig. 2 data), and their Prony approximations based on Eq. (5) with $P = 4$ (red).

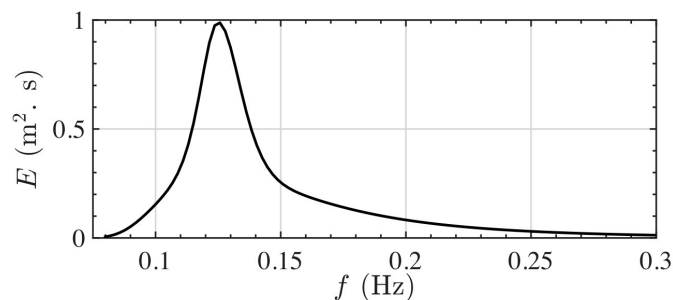


FIGURE 5 – Example of JS wave energy density spectrum for $H_s = 2$ m and $T_p = 8$ s.

peak value. AQWA's results, which are known in the interval $[0.185 - 5.236]$ rad/s are then reinterpolated over the spectral frequencies. For each of these frequencies, wave amplitudes a_n are finally computed, to be used in Eqs. 2 and 3.

III – 2 Non-linear viscous damping

Non-linear damping terms were added to Eqs. 1, as velocity squared empirical terms, to approximate effects of vortex shedding and friction resulting from the boat motions. Due to the box-like hull geometry, the wetted surface area for each dof was simply defined based on the boat overall dimensions, as $S_{w3} = 2D(B + L)$, $S_{w4} = LD$, $S_{w5} = BD$. The drag coefficient for each motion should normally be determined empirically through model testing; however, since model testing has not currently been done yet, drag coefficients were determined using a different method.

The AQWA simulations allow for a correction to the linear damping matrix in order to include nonlinear damping effects through equivalent linearization. The Response Amplitude Operator (RAO) for each dof is then computed in AQWA, based on empirical linear damping corrections that are tuned in order to provide typical and realistic motions for the specific vessel geometry. The resulting RAOs utilizing the linear damping corrections

were used to tune the nonlinear damping coefficients of the current model, which does not apply corrective linear damping terms. Future work will validate the non-linear coefficients based on motions of the scale model system or full physical system. The drag coefficients were iteratively adjusted to produce similar RAO response of the tug boat to that of the provided AQWA simulations, for a range of sample sea states. Figure 6 shows a sample comparison of the RAO calculation of the model for a specified sea state with $H_s = 2$ and $T_p = 8$ s (and for $t_{max} = 100T_p$), compared with the computed RAO from AQWA simulations for the same sea state conditions. In this and other cases, the drag coefficient values used for each dof were : $C_{D3} = 0.5$, $C_{D4} = 2.0$, $C_{D5} = 2.5$.

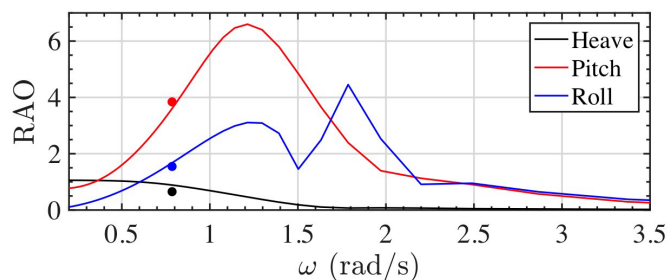


FIGURE 6 – Comparison of heave, roll and pitch RAOs from AQWA simulation (solid lines), for the tug boat in periodic waves, with the RMS values obtained from the nonlinear model simulations (symbols) in irregular waves generated for a JS spectrum with $H_s = 2$ and $T_p = 8$ s, after tuning of non-linear drag parameters. In both cases, waves are incident with $\theta_0 = 25$ deg.

III – 3 Non-linear restoring force

Nonlinear restoring forces may occur in the case of large boat motions, where the assumption of a constant restoring force coefficient $C_{ij}(0)$ does not hold due to changes in the geometry of the submerged vessel. While nonlinear restoring forces may exist due to all motions of the body, it is necessary to have an accurate model of the vessel geometry in order to determine changes in the center of buoyancy due to roll and pitch motions. No accurate CAD model of the tug boat geometry was available, so, only an approximate estimate of the nonlinear heave restoring force coefficient C_{33} was derived based on simple drawings and cross-sections of the boat. Details are left out for brevity.

Assuming the beam cross-section is rectangular at any given depth, the waterplane area is rectangular for any given draft. Hence the nonlinear heave restoring force coefficient was computed as a function of the vessel draft by defining the length of the waterplane area L_{wp} , as a function of draft according to the vessel geometry. With $\xi = \zeta_3 - \eta$:

$$L_{wp}(\xi) = \begin{cases} 18.335 + 3.096(\xi + D_{op}) + 2.797(\xi + D_{op}) & \xi \leq 0.759 - D_{op} \\ 22.125 + 2.979(\xi + D_{op}) & 0.759 - D_{op} < \xi \leq 1.517 - D_{op} \\ 26.3652 & 1.517 - D_{op} < \xi \leq 2.43 \end{cases} \quad (13)$$

with $D_{op} = 0.66$ m the vessel operating draft, and the non-linear heave restoring coefficient reads,

$$C_{33}(\xi) = \rho g B L_{wp}(\xi) \quad (14)$$

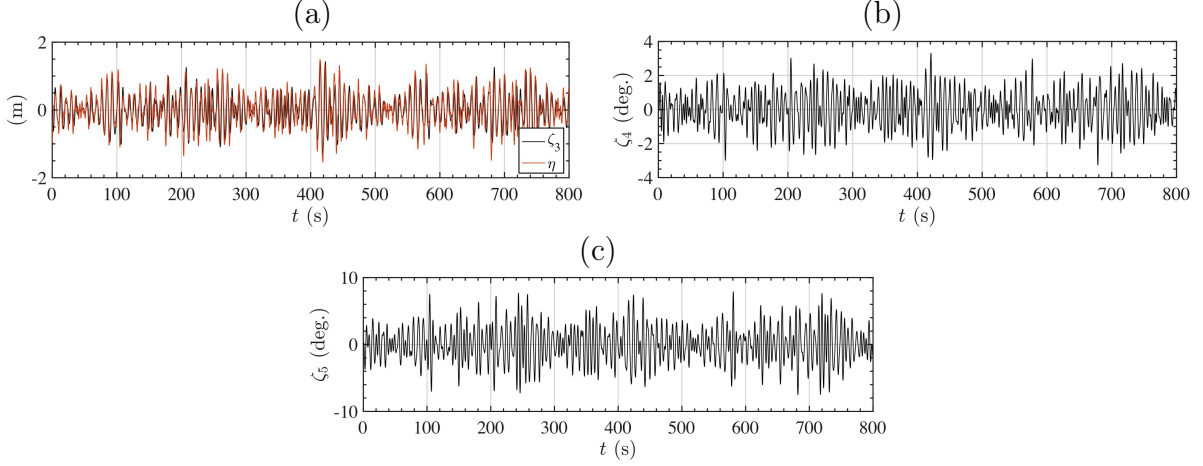


FIGURE 7 – Time series of duration $t_{max} = 100$, $T_p = 800$ s, of warping tug boat motions and wave elevation computed with the nonlinear time domain seakeeping model, in irregular waves generated for a JS spectrum with $H_s = 2$ and $T_p = 8$ s (waves are incident with $\theta_0 = 25$ deg) : (a) heave amplitude and surface elevation ; (b/c) roll/pitch angle.

III – 4 Examples of warping tug motions

For the 3 dofs considered here (heave, roll, pitch) and using $P = 4$ complex Prony parameters for each dof, the nonlinear time domain seakeeping model described by Eqs. (9-12) has 30 first-order coupled ODEs. This system, however, can efficiently be solved using the Matlab ODE solver in a few seconds to simulate long time series of ship motions (e.g., $100T_p$) for any given sea state. Figs. 7 show examples of time series of tug boat motions in heave, roll and pitch, as well as the instantaneous surface elevation $\eta(t)$, for a JS spectrum with $H_s = 2$ and $T_p = 8$ s (here, waves are incident with $\theta_w = 25$ deg).

IV – NN development for sea state prediction

A Neural Network (NN) model is implemented to predict the sea state parameters (H_s, T_p) based on a time series of warping tug boat motions. Before issuing a prediction, the NN is first trained and then validated. This is done based on a large data set of simulated time series of tug motion for many sea states. All NN implementation and simulations are performed using functions in Matlab’s Deep Learning ToolboxTM.

IV – 1 NN model

The NN model is a *Nonlinear Auto-Regressive* (NAR) network with exogeneous inputs (NARX) [2]. It is a recurrent dynamic network, with feedback connections enclosing several layers of the network. By being auto-regressive, the NN allows variables to be regressed also on their past values, possibly nonlinearly, together with new inputs. In addition, such exogeneous inputs are similarly nonlinearly regressed on their past values. The NARX-NN is conceptually represented in Fig. 8 and can simply be formulated as,

$$\mathbf{Y}(t+1) = \mathcal{F} \{ \mathbf{Y}(t), \mathbf{Y}(t-1), \dots, \mathbf{Y}(t-n+1), \mathbf{X}(t), \mathbf{X}(t-1), \dots, \mathbf{X}(t-n+1) \} \quad (15)$$

with \mathbf{Y} a vector of target variables describing the sea state, including significant wave height H_s and peak spectral wave period T_p , and \mathbf{X} a vector of the boat motions in heave (ζ_3), pitch (ζ_4) and roll (ζ_5), all expressed as a function of time t ; n is the length of the

NN Data Sets/ Sea States	t_{max} (s)	H_s range/step	T_p range/step	Nb. Sea States	Nb. 1 s time steps
Training/valid./test.	600	[1-8]/0.2	[5-11]/0.5	490	294,000
Application	60	[1-8]/0.1	[5-11]/0.25	1,000	60,000

TABLE 1 – Parameters of sea states for data sets used in SSNN development and testing.

time series (i.e., number of time samples), and \mathcal{F} is the NARX model, which relates sea state features to target variables. The present NN model has 5 hidden layers of “neurons” acting as both an aggregation component and a transfer function, and 2-time step delays (Fig. 8) [2].

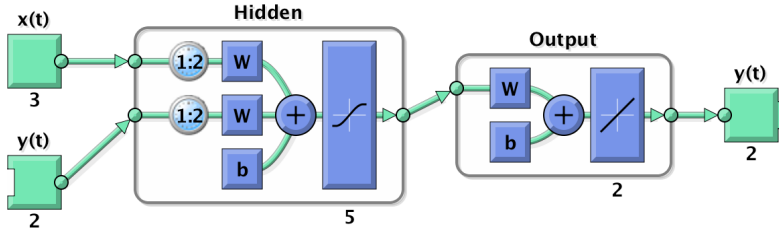


FIGURE 8 – Schematic of the NARX-NN functionality \mathcal{F} for sea-state prediction.

IV – 2 NN training

The NARX-NN is trained to identify a range of sea-states on the basis of the time series of vessel motions simulated with the nonlinear seakeeping model detailed above, for a large number of sea states, each defined by (H_s, T_p) values and represented by a JS spectrum. The vessel is assumed to have no forward speed and all sea states are unidirectional and incident from a constant direction θ_w . For the sake of illustration, $\theta_w = 45$ deg. is used throughout. These assumptions will be removed in future work.

In the training phase, the NN model internal parameters (defining function \mathcal{F}), weights (\mathbf{W}) and bias (\mathbf{B}), are iteratively adjusted based on a heuristic search (so-called “greedy heuristic algorithm”) to minimize errors between simulated and known outputs [2]. The training algorithm stops when errors increase for more than 6 epochs, with an epoch being a measure of the number of times all of the training vectors are used once to update the weights.

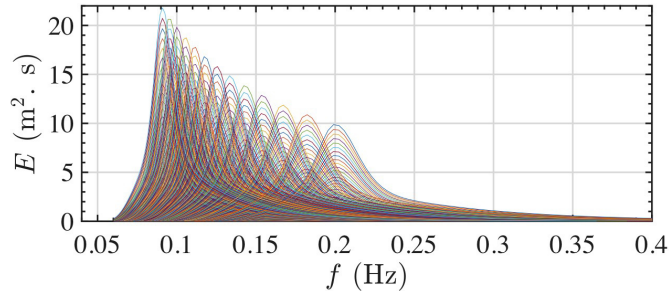


FIGURE 9 – Sea states spectra used as input to train the NN test case (Table 1).

Table 1 provides ranges of NN training parameters for 490 sea-states, combining $H_s \in [1, 8]$ m by 0.2 m increments and $T_p \in [5, 11]$ s by 0.5 s increments; Fig. 9 shows all the corresponding JS spectra. For each sea state, the seakeeping model is run to simulate the

NN process	Relative sample size (%)	RMS	R^2
Training	55	$2.26 \cdot 10^{-3}$	0.9997
Validation	15	$1.81 \cdot 10^{-3}$	0.9997
Testing	30	$2.41 \cdot 10^{-3}$	0.9997

TABLE 2 – Root Mean Square error (RMS) and determination coefficient (R^2) for the 3 NN sampled data sets.

time series of vessel motion in heave, pitch, and roll; all individual sea state time series have the same duration $t_{max} = 600$ s and are re-interpolated on a fixed time step $\Delta t = 1$ s. Fig. 7 shows an example of an individual time series computed with the seakeeping model for 1 sea state. Data and results for all sea states are concatenated into a single time series, for each parameter or boat motion, each with $n = 490 \times 600 = 294,000$ data points. The NN is trained using a randomly selected sample of 55% of these data points, with 15% and 30% set aside to be used later for the NN validation and application, respectively (Table 2). A Levenberg-Marquardt algorithm is used for training [2].

Table 2 shows overall results of the NN training. An excellent agreement between output and target data is obtained, with a determination coefficient $R^2 = 0.9997$ (representing the fraction of total variance in the training sample explained by the NN). One can see that a measurable error on the predicted H_s only occurs during the first few seconds, when the sea-state parameters abruptly change, between one of the 490 sea states to the next. A highly accurate prediction is observed for later times.

IV – 3 NN validation and testing

The NN validation stage uses an independent data set from that used in training (15% of the initial sample; Table 2), to prevent the model from overfitting. In the validation stage, weights in the NN model function \mathcal{F} are no longer adjusted, but other NN parameters are iteratively refined. The validation stage generalizes the NN model, such that in the present case, it will accurately predict sea states not represented in the training sample. Table 2 shows that the NN prediction errors are slightly decreased as a result of the validation stage, with a minimum RMS error of 1.81×10^{-3} , here at 55 epochs.

In the NN testing stage, the remaining 30% of the initial sample were used to test the model. The NN free parameters, weights, and bias are fixed at the values obtained during the training/validation stages for testing. Table 2 shows that prediction errors on this unused sample are as low as for the other stages, which confirms the NN’s ability to predict sea state parameters. This is further verified in the next section.

IV – 4 NN application to predict sea state parameters

A final assessment of the NN’s ability to predict sea state is done using a fully independent “application” data set also built with the seakeeping model, for which Table 1 shows that the same (H_s, T_p) ranges is covered, but in 50% smaller increment, yielding 1,000 sea states. However, much shorter time series of the vessel motion, with $t_{max} = 60$ s, are generated with a 1 s time step, yielding $n = 60,000$ long single time series. The RMS error of the NN prediction of sea state parameters in the application data set is shown in Fig. 10 in dimensional units. As before, the accuracy of the NN prediction is very good.

It is important to note that here, randomly changing the sea state every 60 s not only

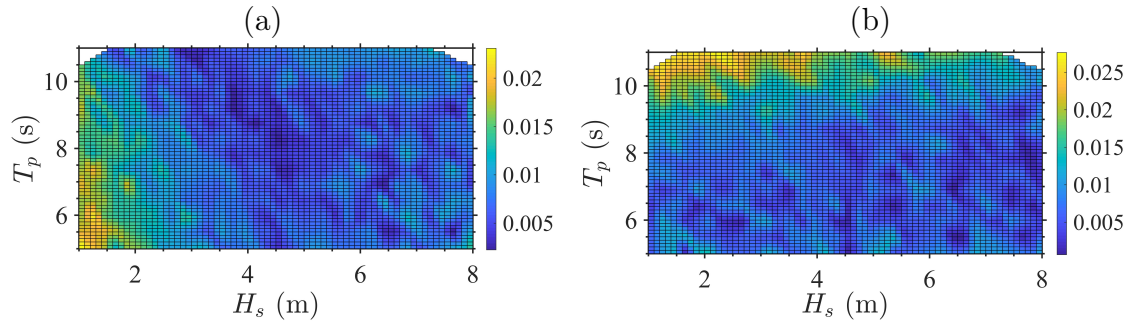


FIGURE 10 – RMS error of NN prediction of application data set parameters (Tables 1 and 2) : (a) H_s (in m); and (b) T_p (in s), as a function of target sea state values (H_s, T_p).

demonstrates the NN’s ability to predict current sea state conditions using a very short time series of boat motion, but its adaptability to rapidly changing sea state conditions.

V – Conclusions

A NN model was implemented and validated to predict sea state parameters, based on time series of ship motion. The latter were obtained from realistic seakeeping simulations, but actual data from model testing and field measurements will be used in future phases of the project. Current results demonstrate the excellent ability of the trained NN model to predict sea state parameters when provided with short time series (60 s) of boat motions. This is very promising but will need to be confirmed using short time histories of actual boat motion data from a sensor (tank or field), which will include noise.

In future work, model testing in a tow tank will provide actual boat motion time series in controlled sea states and will be used to validate the seakeeping model and NN training procedure; in particular viscous damping terms will be calibrated. Tests will be performed without and with a forward speed. The seakeeping model will be generalized to use more arbitrary directional sea states and include the boat forward speed, and the present study will be repeated.

Acknowledgements This material is based upon work supported by the Naval Facilities Engineering and Expeditionary Warfare Center under Contract No. N3943018C2020. Any opinions, findings and conclusions or recommendations expressed in this material are those of the authors and do not necessarily reflect the views of the Naval Facilities Engineering and Expeditionary Warfare Center. The authors gratefully acknowledge support for this work through a subcontract from Create Inc.

Références

- [1] A. Babarit and A. H. Clément. Wave-induced mass transport in water waves. *Applied Ocean Res.*, 28 :77–91, 2006.
- [2] C. M. Bishop. *Neural networks for pattern recognition*. Clarendon Press, Oxford, 1995.
- [3] S. Grilli, A. Grilli, S. Bastien, R. Sepe Jr., and M. Spaulding. Small buoys for energy harvesting : Experimental and numerical modeling studies. In *21st International Off-shore and Polar Engineering Conference*, pages 598–605, Maui, HI, USA, June 2011. ISOPE.